RSC Advances

Intrinsic polyphenol oxidase-like activity of gold@platinum nanoparticles

Journal:	*RSC Advances*
Manuscript ID:	RA-ART-04-2015-007636.R2
Article Type:	Paper
Date Submitted by the Author:	09-Jul-2015
Complete List of Authors:	Lee, Jo-Won; Chung-Ang Univ, Yoon, Sohee; Chung-Ang Univ, Lo, Y; University of Maryland, College Park, Department of Chemistry and Biochemistry Wu, Haohao; U.S. Food and Drug Administration, Center for Food Safety and Applied Nutrition Lee, Sook-young; Chung-Ang Univ, Moon, B. K.; Chung-Ang University, food and nutrition

Intrinsic polyphenol oxidase-like activity of gold@platinum nanoparticles

Jo-Won Lee[a], Sohee Yoon[a], Y. Martin Lo[b], Haohao Wu[c], Sook-Young Lee[a], BoKyung Moon[a]

[a] Department of Food & Nutrition, Chung-Ang University, Seoul 156-756, Korea

[b] Biointellipro LLC, Ashton, MD, 20860, USA

[c] College of Food Science and Engineering, Ocean University of China, Shandong Province 266003, China

Corresponding author:

BoKyung Moon

Department of Food &Nutrition, Chung-Ang University, Seoul 156-756, Korea

Tel: +82-31-670-3273: Fax: +82-31-676-8741

E-mail: bkmoon@cau.ac.kr

Abstract

Metal nanoparticles (NPs) have received considerable attention in recent years for their unique properties and potential applications in catalysis. However, few studies have employed an integrated approach to investigate the enzyme mimetic activities of metal NPs. The aim of the present study was to evaluate the enzyme mimetic activity of gold@platinum (Au@Pt) NPs. Specifically, the lipoxygenase (LOX), glutathione reductase (GR), glutathione peroxidase (GPx), and polyphenol oxidase (PPO) activities of Au@Pt NPs were examined. The results showed that Au@Pt NPs exhibited PPO mimetic activity over a wider range of pH values and temperatures compared with PPO. Kinetic analysis showed that Au@Pt NPs exhibited higher affinity for certain substrates than the natural enzyme PPO. Furthermore, we also determined the catalytic activity of Au@Pt NPs in the autoxidation of phenol substrates, including pyrogallol, 3,4-dihydroxy-L-phenylalanine, and catechol by electron spin resonance.

Keywords: Au@Pt nanoparticles, enzyme mimetics, polyphenol oxidase, ESR

Introduction

Natural enzymes have been widely used in food processing, the medicinal and chemical industries, and agriculture because of their high substrate specificities and high catalytic efficiency under mild conditions.[1-4] However, they have intrinsic limitations such as high costs for preparation and purification, low stability caused by denaturation, and limitation for large-scale applications.[5] Therefore, with advances in artificial enzyme mimics, it has become possible to find enzyme alternatives that have advantages with respect to cost, easy storage, and flexibility, as well as high substrate specificities and stability even under rigorous conditions.

Metal nanoparticles (NPs) have received considerable attention in recent years because of their unique properties and potential applications as enzyme alternatives.[1] There have been reports that some NPs, including Co_3O_4,[2] BSA-stabilized Au clusters,[3] Fe_3O_4,[6] CuS,[7] and platinum NPs,[8] showed potential as peroxidase (POD) mimetics. Previous studies have shown that gold@platinum (Au@Pt) NPs act like an ascorbic acid oxidase or peroxidase.[5,9]

POD is an oxidoreductase involved in enzymatic browning, since diphenols may function as reducing substrates in its reaction.[10] Au@Pt NPs demonstrate catalase-like activity, which was determined by electron spin resonance (ESR).[11] In addition, Au@Pt nanorods are kinetically similar to AA oxidase during AA oxidation.[5] Therefore, metal nanostructure could be considered as a new class of enzyme mimics with merits such as stability under denaturation and deactivation conditions. They also have additional advantages with respect to costs and tunability of catalytic activities that enable their use in many enzyme-related applications.[8] However, their enzyme mimetic activities are strongly dependent on their size and solubility.[1,6] It has been reported that the percentage mole ratio of

Pt-to-Au changed the H_2O_2 scavenging effect of NPs, and their enzymatic activity decreased with the increase in the size of NPs.[12, 13]

Enzymatic browning is considered one of the main problems of postharvest fruits and vegetables, especially in damaged tissues. Therefore, enzyme activity causes practical limitation for the handling, storage, and processing of fruits and vegetables.[14-17] Enzymatic browning caused by polyphenol oxidase (PPO) activity is a major problem undermining the quality of produce post-harvest. However, browning by PPO is not always an undesirable reaction: for example, it is responsible for the development of a brown color during the processing of black tea and cocoa.[18]

In this study, we aimed to screen the enzyme mimetic effects of Au@Pt NPs and to evaluate the possibility of their use as enzyme alternatives. For this purpose, the lipoxygenase (LOX)-like, glutathione reductase (GR)-like, and glutathione peroxidase (GPx)-like activities of Au@Pt NPs were evaluated. In addition, PPO-like activity was monitored by ESR and enzyme kinetic parameters were evaluated.

Experimental

Materials

Linoleic acid, pyrogallol, cytosol, catechol, nitro-blue tetrazolium (NBT), 3,4-dihydroxy-L-phenylalanine (L-DOPA), β-nicotinamide adenine dinucleotide phosphate, reduced tetra (cyclohexylammonium) salt (NADPH), PPO (E.C. 1.14.18.1 from mushroom), and the spin label 3-carbamoyl-2,2,5,5-tetramethyl-3-pyrroline-1-yloxyl (CTPO) were purchased from Sigma-Aldrich Co (St. Louis, MO, USA).

Characterization of nanoparticles

Au@Pt NPs were purchased from NanoSeedz™ (Hong Kong, China). The Pt:Au ratio was 1:4, and the Au core was 96 × 40 nm (length × diameter). The zeta potential of NPs was 17.93 mV and the thickness of the Pt shell was approximately 3 nm. The NP surface was positively charged and conjugated with cetyltrimethyl ammonium bromide (Fig. 1).

Enzyme-mimetic activity of Au@Pt NPs

The LOX activity of Au@Pt NPs was measured by the method of Yi *et al*. with a slight modification. Linoleic acid (10 mM) in phosphate buffer (0.2 mM, pH 7.0) was diluted 50 times.[19] Diluted linoleic acid solution (2.9 mL) with 0.1 mL sample solution was incubated at 25 °C for 4 h. The LOX activity is expressed as the change in absorbance at 234 nm.

The GR activity of Au@Pt NPs was determined according to Carlber and Mannervik's method with slight modifications.[20] In brief, 0.5 mL of ethylenediaminetetraacetic acid (EDTA)/potassium phosphate buffer (2 mM/0.2 mM, pH 7.0), 0.05 mL of NADPH, 0.05 mL of oxidized glutathione solution (20 mM), and 0.4 mL ultrapure deionized water were placed in a cuvette, and incubated at 30 °C after the addition of 0.04 mL of sample. The decrease in absorbance at 340 nm was monitored for 3 min using a spectrophotometer (Bio Tek Instruments, VT, USA). The GR activity is expressed as 1 μmol NADPH per min under the assay condition.

The GPx activity of Au@Pt NPs was determined according to the method described by Tappel with some modifications.[21] The reaction mixture, which consisted of 1290 μL of 50 mM potassium phosphate buffer (5 mM EDTA), 50 μL of 8.4 mM NADPH, 5 μL of NaN_2, and 50 μL of glutathione (GSH) was mixed with 50 μL sample solution. The reaction solution was vortexed and incubated at 25 °C for 5 min, followed by addition of H_2O_2. The decrease in absorbance at 340 nm was monitored for 2 min on a spectrophotometer (Bio Tek Instruments). GPx activity was defined as the amount of oxidized NADPH per min.

The PPO-like activity of Au@Pt NPs was determined using catechol as a substrate by measuring the increase in absorbance at 420 nm.[22] The total reaction volume was 300 μL, which consisted of 60 μL of the enzyme or Au@Pt NPs, 180 μL of 1/15 mM sodium phosphate buffer (pH 7.0), and 60 μL substrate. The negative control contained only 180 μL of 1/15 mM sodium phosphate buffer (pH 7.0) and 60 μL of substrate, and distilled water. The reaction solution was incubated at 25 ℃ for 5 min. [22]

PPO mimetic activity of Au@Pt NPs

Effect of pH and temperature. The PPO-like activity of Au@Pt NPs at different pH and temperatures was measured using the methods described above. To determine optimum pH, 100 mM hydrochloric acid-potassium chloride (pH 1.0), glycine-HCl (pH 2.0–3.0), acetate buffer (pH 4.0–5.0), phosphate buffer (pH 6.0–8.0), Tris-HCl (pH 9.0–10.0), monosodium phosphate-NaOH (pH 11.0), and potassium chloride-NaOH buffer (pH 12.0) solutions were used.[16] The reaction solution included 60 μL of 15 units of PPO or 50 μg L^{-1} of Au@Pt NPs, 180 μL of buffer solution, and 60 μL of 10 mM catechol. Absorbance at 420 nm was monitored at 25 ℃ for 30 min. The optimum pH values obtained from this assay were used in all subsequent experiments. To examine the influence of incubation temperature on the relative activity of 15 units of PPO or 50 μg L^{-1} of Au@Pt NPs, catalytic reactions were monitored by the change of absorbance at 420 nm at different temperatures from 0 to 60 ℃ under the optimum pH.[14] To monitor the stability of the PPO-like activity of Au@Pt NPs, the reaction was monitored at different pH and temperature for 120 min.

Kinetic analysis and substrate specificity. The reaction kinetics for the catalytic oxidation of substrates by Au@Pt NPs or PPO were determined by monitoring the absorbance changes within a 1 min interval.[1] In brief, 60 μL of 15 units of PPO or 50 μg L^{-1} Au@Pt NPs was

mixed with 60 μL of substrates in 180 μL reaction buffer (0.2 M acetate buffer, pH 5), and the absorbance change at 420 nm for catechol, 475 nm for L-DOPA, and 320 nm for pyrogallol was monitored at 1 min intervals at 40 °C.[1] The kinetics were determined using the Michaelis-Menten constant, which is defined as follows:

$$V = (\ Vmax \times [S])/(Km + [S])$$

Where V is the initial velocity, $Vmax$ is the maximum reaction velocity, S is the concentration of substrate, and Km is the Michaelis constant.

Oxidation of phenolic substrates catalyzed by Au@Pt NPs determined with ESR

ESR spin label oximetry was used to determine the oxygen consumption during autoxidation of pyrogallol, L-DOPA, and catechol catalyzed by Au@Pt NPs. The reaction mixture contained 0.1 mM CTPO and 5 mM pyrogallol, L-DOPA, or catechol in 100 mM phosphate-buffered saline (PBS) (pH 7.4) with or without the presence of 15 μg L^{-1} Au@Pt NPs. Samples were placed in 50 μL glass capillary tubes and sealed at both ends. Data collection began 1 min after sample mixing, and the spectra were recorded on a Bruker EMX ESR spectrometer (Billerica, MA, USA) using the following settings: 1 mW microwave power, 0.04 G field modulation, and 5 G scan range.[23]

The oxygen consumption of Au@Pt NPs, PPO, and apple juice was also determined. The reaction mixture contained 0.1 mM CTPO and 25 μg L^{-1} Au@Pt NPs, 15 units of PPO, or 100 μL apple juice with or without AA (0.1%) and Au@Pt NPs (25 μg L^{-1}) in 100 mM PBS (pH 7.4). Data collection began 4 min after sample mixing and all other conditions were the same as those described above.

Measurement of Au@Pt NP or PPO reaction products by high-performance liquid chromatography (HPLC)

Reaction mixtures consisted of L-DOPA (10 mM) and PPO (50 unit) or Au@Pt NPs (50 μg L^{-1}) in a 1/15 mM sodium phosphate buffer (pH 7.0) incubated at 25 °C for 2 h. Reaction products were detected at 5 min and 1 and 2 h on an analytical HPLC apparatus (L-2130 pump with L-2200 auto sampler, L-2300 column oven, and L-2400 UV detector; Hitachi, Tokyo, Japan) with a reversed phase Capcell Pak C_{18} (250 × 4.6 mm; inner diameter: 5 μm; Shiseido, Tokyo, Japan) column. Solvent A was prepared by adding concentrated formic acid (0.1%) to deionized water and Solvent B was prepared by adding formic acid (0.1%) to HPLC-grade acetonitrile. The mobile gradient was as follows: 0–30 min, linear gradient from 100% solvent A to 75% solvent B; 30–40 min, linear gradient to 100% solvent B. The flow rate was constant at 1.0 mL min^{-1}.[24]

Statistical analysis

Quantitative data are expressed as the mean ± standard deviation (SD) of triplicate measurements. Each set of experimental data was compared with the results of one-way analysis of variance (ANOVA) and Duncan's multiple-range test ($p < 0.05$) using SAS version 8.0 for Windows (SAS Institute; Cary, NC, USA).

Results and discussion

Enzyme activity of Au@Pt NPs

LOX activity. LOX is an enzyme found in many plants and animals. It catalyzes the oxygenation of polyunsaturated fatty acids to form fatty acid hydroperoxides, and linoleic and linolenic acid are the major polyunsaturated fatty acids in plant tissues.[25] LOX plays a role in the production of off-flavors in soybeans[26] and many vegetables such as tomatoes. However, LOX-produced odorant compounds are desirable in cucumber products.[27-29] The

LOX activity of Au@Pt NPs is shown in Fig. 2. In the Au@Pt NP concentration range of 2.5–125 μg L^{-1}, LOX activity was 3.2803–3.2827 initially, and 3.2824–3.2988 and 3.2826–3.2897 after 2 h and 4 h, respectively (Fig.2).

The Au@Pt NPs exhibited LOX activity, whereas the negative controls did not show any LOX activity. The results showed that Au@Pt NPs have potential as alternative LOX mimics, although the activity was relatively low at 125 μg L^{-1}.

GR activity. The GR activity of Au@Pt NPs was measured in the concentration range of 0.025–250 μg L^{-1}. Compared with the negative control, the Au@Pt NPs did not show significant changes in GR activity (data not shown). Therefore, we considered that Au@Pt NPs do not have GR activity.

GPx activity. GPx activity, which reduces H_2O_2 and lipid hydroperoxide, of Au@Pt NPs is shown in Fig. 3, which was measured at the concentration range of 0.025–250 μg L^{-1}. Although Au@Pt NPs showed GPx activity at 2.5 μg L^{-1} in preliminary experiments, the activity was very low. There was no GPx activity detected when the concentration of Au@Pt NPs was higher than 2.5 μg L^{-1}.

PPO mimetic activity. As shown in Fig. 4(A), Au@Pt NPs could catalyze the oxidation of substrates and change the typical color of the PPO substrate solution. L-DOPA, catechol, pyrogallol and tyrosine, were oxidized, producing coppertone, gray, yellow and deep gray solutions, respectively. These results indicate that the Au@Pt NPs have PPO mimetic activity toward typical PPO substrates. The PPO mimetic activity of Au@Pt NPs at different concentrations was also determined using catechol as a substrate by measuring the increase in absorbance at 420 nm (Fig. 4(B)). The results showed that Au@Pt NPs have PPO mimetic

activity in the concentration range of 12.5–250 μg L^{-1}, and at concentrations higher than 125 μg L^{-1}, the NPs showed activity greater than 110 units of PPO (E.C. 1.14.18.1 from mushroom). Our results showed that the catalytic activity of Au@Pt NPs was similar to that of the natural enzyme PPO.

Enzyme mimetic activity of Au@Pt NPs

Effect of pH and temperature. The PPO mimetic activity of Au@Pt NPs and PPO was measured in the pH range of 1.0 to 12.0 and in the temperature range of 0 to 60 °C. The reaction solution pH- and temperature-dependent response curves are shown in Fig. 5(A) and (B), respectively. The results showed that the optimal pH is 6.0 and 5.0 for Au@Pt NPs and PPO, respectively. The usual pH dependence for enzyme activity is represented as a bell-shaped curve. The optimum pH of PPO varies from approximately 4.0 to 7.0, depending on the origin of the material, extraction method, and substrate.[17, 30] In addition, the optimum pH of plant PPOs is around 6 to 7.[31,32] The PPO mimetic activity of Au@Pt NPs was compared with that of 15 units of PPO in the same temperature range. The optimal temperatures were 20 °C and 40 °C for Au@Pt NPs and PPO, respectively (Fig. 5(B)). Jiao *et al.*[1] reported that CeO_2 NPs showed peroxidase-like activity, and their optimum temperature was different from that of peroxidase. Thus, we considered pH 6.0 and 20 °C as the optimum condition for the PPO mimetic activity of Au@Pt NPs.

The stability of the Au@Pt NPs was measured over a wide range of pH and temperature (Fig. 6). Au@Pt NPs were incubated at a range of pH and temperatures for 120 min. In general, the catalytic activity of natural enzymes is sensitive to environmental conditions and shows low stability due to denaturation.[33-35] In contrast, the catalytic activity of the Au@Pt NPs showed stability over a wide range of pH (1–12) and temperature (0–60 °C). These results showed that the robustness of the Au@Pt NPs make them applicable for

use under harsh conditions. Zhou *et al*. reported that Au@Pt nanorods are much more stable catalysts than ascorbic acid oxidase (AAO) over a wide range of pH values. [5] In addition, metal NPs as peroxidase mimetics have been demonstrated to be suitable for various applications, including in the biomedicine and environmental chemistry fields.[1, 6-11, 36]

Kinetic analysis and substrate specificity. The kinetic parameters of enzyme mimetic Au@Pt NPs are shown in Table 1. When catechol and L-DOPA were used as substrates, the *Km* values of PPO were much lower than those of PPO with pyrogallol. In general, *Km* is identified as an indicator of an enzyme's affinity to substrates, and because L-DOPA showed the lowest *Km* values, it was considered to be the preferred substrate. In the oxidation of all substrates, Au@Pt NPs exhibited lower catalytic activity but higher affinity to the substrates, especially to catechol and pyrogallol, compared with PPO. According to He *et al*. the active site for Au@Pt NPs are Pt nanodots which have approximately below 5 nm of diameter.[11] Therefore, the large surface area of Pt nanodots might promote electron transfer during the oxidation reaction.[11, 35] The catalytic activity of Au@Pt NPs over PPO towards catechol, L-DOPA, and pyrogallol demonstrated their enzymatic mimetic activity.

Oxidation of phenolic substrates catalyzed by Au@Pt NPs using ESR oximetry

Due to the hyperfine interaction of unpaired electrons with the nitrogen nucleus, CTPO displays three ESR lines, each of which is further split into another group of lines as a result of proton super hyperfine interactions. The resolution of the super hyperfine structure of the low-field ESR line of CTPO is dependent on the oxygen concentration in the solution. Fig.7 shows the spectrum evolution of CTPO during the autoxidation of pyrogallol, L-DOPA, and catechol in a closed chamber. The time-dependent increase in super hyperfine splitting indicates the disappearance of oxygen in the solution. The presence of Au@Pt NPs increased

the oxygen consumption rates of pyrogallol, L-DOPA, and catechol, which confirmed the catalytic role of Au@Pt NPs in the autoxidation of these phenol substrates. Pyrogallol displayed the highest autoxidation rate among these three phenol substrates. Therefore, the results obtained from the study of the oxidation of phenolic substrates catalyzed by Au@Pt NPs using ESR oximetry demonstrated that Au@Pt NPs exhibit PPO mimetic activity.

ESR was also used to compare oxygen consumption of Au@Pt NPs and PPO in apple juice with naturally occurring PPO (Fig. 8). In the spectrum of CTPO during autoxidation of apple juice (Fig. 8A), similar ESR signals were observed for Au@Pt NPs and PPO (Fig. 8B, C). The ESR signal for apple juice nearly disappeared when AA was added (Fig. 8D); however, the signal increased when Au@Pt NPs were added to the apple juice in the presence of AA (Fig. 8E). These results suggest that Au@Pt NPs function in a manner similar to PPO in apple juice.

Evaluation of reaction products generated by PPO or Au@Pt NPs

Reaction products generated by PPO and Au@Pt NPs with L-DOPA were compared by HPLC analysis of the reaction mixture. There were no peaks detected for L-DOPA after a 2-h incubation in the absence of PPO and Au–Pt NPs (Fig. 9A). Enzymatic reactions of L-DOPA with Au@Pt NPs or PPO produced peaks with the same range of retention times and similar shapes after a 5-min incubation (Fig. 9B); after 1 and 2 h of incubation, Au@Pt NPs and PPO reaction products detected at a given retention time differed from those detected at 5 min (Fig. 9C, D). Moreover, Au@Pt NPs and PPO reaction products decreased over time (Fig. 9B, C). Although the products could not be identified, these results indicate that Au@Pt NPs oxidize L-DOPA and generate products that are similar to those produced by PPO and therefore have PPO-like activity.

Conclusion

In this study, the results obtained indicated that the Au@Pt NPs exhibit intrinsic PPO-like activity. Compared to PPO, the Au@Pt NPs showed PPO mimetic activity over a wider range of pH and temperature. The kinetic analysis results demonstrated that the Au@Pt NPs have higher affinity to the substrates compared to PPO. In addition, the Au@Pt NPs as a mimetic PPO showed several advantages over natural enzyme, such as low-cost, ease of preparation and stability. Based on the results of this study, Au@Pt NPs can be considered to be stable and effective mimetic of PPO and show potential for application as a new nanoparticle-based indicator control system for monitoring oxidative reactions under different conditions.

Acknowledgements

We thank Dr. Jun-Jie Yin for his valuable comments on this manuscript. This research was supported by the Basic Science Research Program through the National Research Foundation of Korea (NRF) funded by the Ministry of Science, ICT and Future Planning (NRF-2012R1A1A3012885).

Notes and references

1. X. Jiao, H. Song, H. Zhao, W. Bai, L. Zhang and Y. Lv, *Anal. Methods*, 2012, **4**, 3261.
2. J. Mu, Y. Wang, M. Zhao and L. Zhang, *Chem. Commun*, 2012, 48, 2540.
3. X. X. Wang, Q. Wu, Z. Shan and Q.M. Huang, *Biosens. Bioelectron*, 2011, **26**, 3614.
4. J. Liu, X. Hu, S. Hou, T. Wen, W. Liu, X. Zhu and X. Wu, *Chem. Commun*, 2011, **47**, 10981.
5. Y. T. Zhou, W. He, W. G. Wamer, X. Hu, X. Wu, Y. M. Lo and J. J. Yin, *Nanoscale,* 2013, **5**, 1583.
6. L. Gao, J. Zhuang, L. Nie, J. Zhang, Y. Zhang, N. Gu, T. Wang, J. Feng, D. Yang, S. Perrett and X. Yan, *Nat. Nanotechnol*, 2007, 2, 577–583.
7. W. W. He, H. Jia, X. Li, Y. Lei, J. Li, H. Zhao, L. Mi, L. Zhang and Z. Zheng, *Nanoscale,* 2012, 4, 3501–3506.
8. Y. Dong, Y. Chi, X. Lin, L. Zheng, L. Chen and G. Chen, *Phys. Chem. Chem. Phys*, 2011, **13**, 6319.
9. J. Liu, X. Hu, S. Hou, T. Wen, W. Liu, X. Zhu, J.J. Yin and X. Wu, *Sens. Actuators, B*, 2012, **166–167**, 708.
10. M. Chisari, R. N. Barbagallo and G. Spagna, *J. Agric. Food Chem*, 2007, **55**, 3469-3476.
11. W. He, Y. Liu, J. Yuan, J. J. Yin, X. Wu, X. Hu, K. Zhang, J. Liu, C. Chen, Y. Ji, Y. Guo, *Biomaterials,* 2011, **32**, 1139.
12. M. Kajta, K. Hikosaka, M.Iitsuka, A. Kanayama, N. Toshima and Y. Miyamoto, *Free Radical Re*, 2007, **41**, 615.
13. J. N. Talbert and J. M. Goddard, *Food Bioprod Process*, 2013, **91**, 693.
14. Y. Z. Doğru and M. Erat, *Food Res Int*, 2012, **49**, 411.

15. O. Lamikanra and M. A. Waton, *J Agric Food Chem*, 2001, **66,** 1283.

16. C. Queiroz, A. J. R. Silva, M. L. M. Lopes, E. Fialho, V. L. Valente-Mesquita, *Food Chem*, 2011, **125**, 128.

17. S. Doğan, P. Turan and M. Doğan, *Process Biochem,* 2006, **41**, 2379.

18. V. C. Quesnel and K. Jugmohunsingh, *J Sci **Food** Agric,*1970, **21**, 537.

19. H. Yi, M. Yi and H. T. Choe, *J. Plant Biology*, 2005, 48, 429.

20. C. Carlberg and B. Mannervik, *Meth Enzymol*, 1985, **113**, 484.

21. A.L. Tappel, *Meth Enzymol*, 1978, **52**, 506.

22. E. Mustafa, S. Halis and K. O. Irfan, *Food Chem*, 2006, **95**, 503.

23. Y. T. Zhou**,** J. J. Yin and Y. M. Lo, *Magn Reson Chem*. 2011, **49**, 105.

24. T.N. Kentaro, H. Tomoko, O. Takeshi and T. Takao, *Biochem Biophys Res Commun*, 2006, **343**, 15.

25. T. Baysal and A. Demirdöven, *Enzyme Microb Technol*, 2007, **40**, 491.

26. S. C. Sheu and A. O. Chen , *J Food Sci,*1991, **56**, 448.

27. C. M. Shook, T. H. Shellhammer, S. J. Schwartz , *J Agric Food Chem*, 2001, **49**, 664.

28. Q. Li, X. Wu, H. Li, M. Hang and D, Zhu, *J. Northeast Agric. Univ,* 2008, **39**, 62.

29. L. Zhao, S. Wang, F. Liu, P. Dong, W. Huang, L. Xiong and X. Liao, *Innov Food Sci Emerg Technol,* 2013, **17**, 27.

30. Y. M. Jiang, Z. Giora and F. Yoram, *Postharvest Biol Technol*, 1997, **10**, 221.

31. E. Arias, J. González, R. Oria and P. Lopez-Buesa, *J Food Sci*, 2007, **72**, 422.

32. F. Artés, M. Castañer and M. I. Gil, *Food Sci Technol Int*, 1998, **4**, 377.

33. X . Hu, A. Sarn, S, Hou, T. Wen, Y. Ji, W. Liu, H. Zhang, W. He, J.J .Yin and X.Wu, *RSC Adv,* 2013, **3**, 6095.

34. W. Chen, J. Chen, A. L. Liu, L.M. Wang, G.W. Li and X.H Lin, *ChenCatChem,* 2011, **3**, 1151.

35. W.B. Motherwell, M. J. Bingham and Y. Six, *Tetrahedron*, 2001, **57**, 4663.

36. J. Fan, J.J Yin, B. Ning, X. Wu, Y. Hu, M. Ferrari, G. J. Anderson, J. Wei, Y. Zhao and G. Nie, *Biomaterials*, 2011, 32, 1611-1618.

Table 1. Comparison of the kinetic parameters for polyphenol oxidase and Au@Pt NPs.

Substrate	*Km* (mM)		*Vmax* (mol L^{-1} min^{-1})	
	PPO*	Au@Pt NPs	PPO	Au@Pt NPs
Catechol	3.05×10^2	1.29×10^2	36.05×10^0	13.97×10^0
L-DOPA	7.37×10^0	6.70×10^0	2.10×10^0	9.91×10^0
pyrogallol	3.11×10^3	6.51×10^2	2.08×10^2	44.38×10^0

*PPO; polyphenol oxidase; *Km*, Michaelis constant; *Vmax*, maximum reaction rate. Oxidation activity of Au@Pt NPs was determined with catechol, L-DOPA, and pyrogallol substrates.

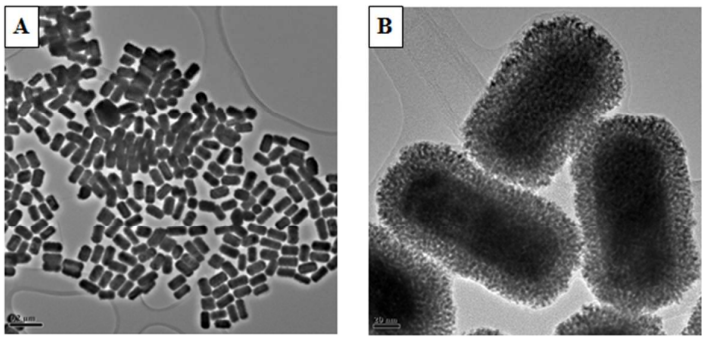

Fig. 1 HR-TEM images (A) showing morphology and core-shell structure of Au@Pt nanoparticles (NPs). (B) high-magnification images showing Au@Pt nanostructures.

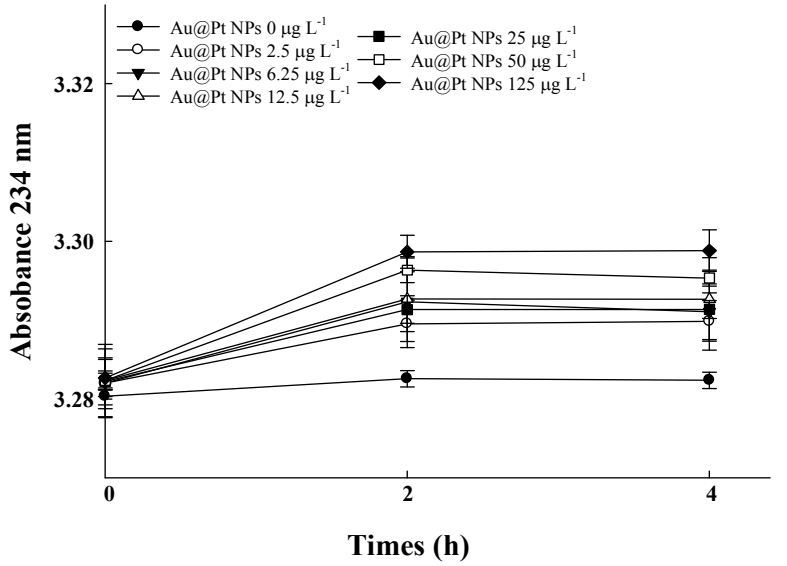

Fig. 2 Lipoxygenase (LOX)-like activity of Au@Pt nanoparticles (NPs) at different Au@Pt NP concentrations. The LOX activity in the Au@Pt NPs was measured at 234 nm. The data are presented as mean ± SD (n = 3).

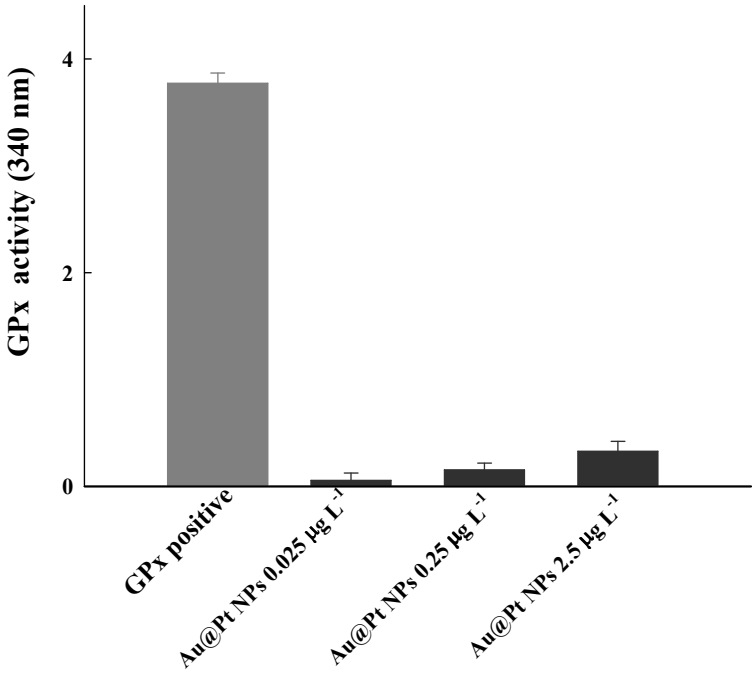

Fig. 3 Glutathione peroxidase (GPx)-like activity of Au@Pt nanoparticles (NPs). The GPx activity of Au@Pt NPs was compared with that of bovine erythrocytes as a positive control. The data are presented as mean ± SD (n = 3).

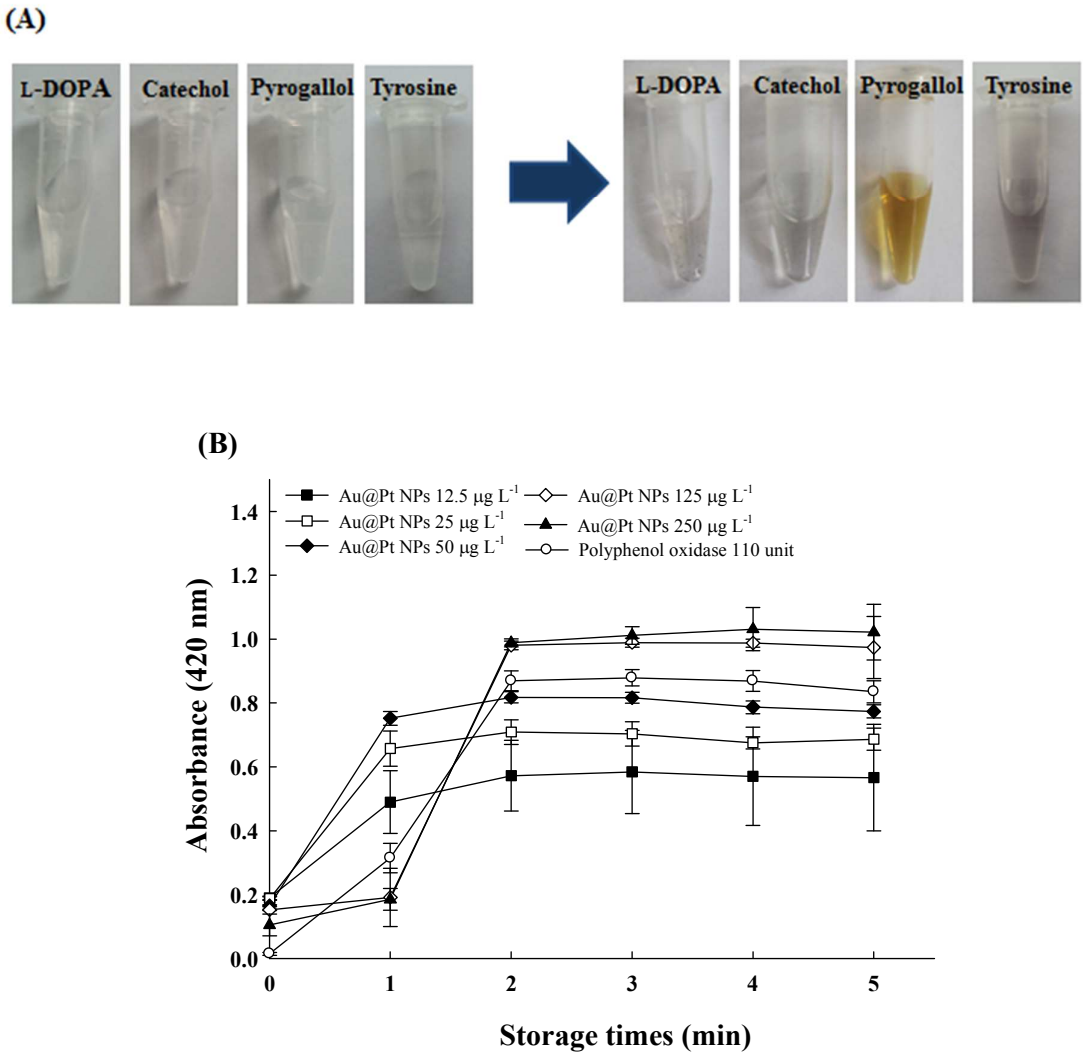

Fig. 4 Polyphenol oxidase-like activity of Au@Pt nanoparticles (NPs). (A) Color evolution of L-DOPA, catechol, pyrogallol and tyrosine oxidation catalyzed by Au@Pt NPs. (B) The time-dependent absorbance changes at 420 nm for 110 units of PPO or 12.5–250 μg L^{-1} of Au@Pt NPs. The data are presented as mean ± SD (n = 3).

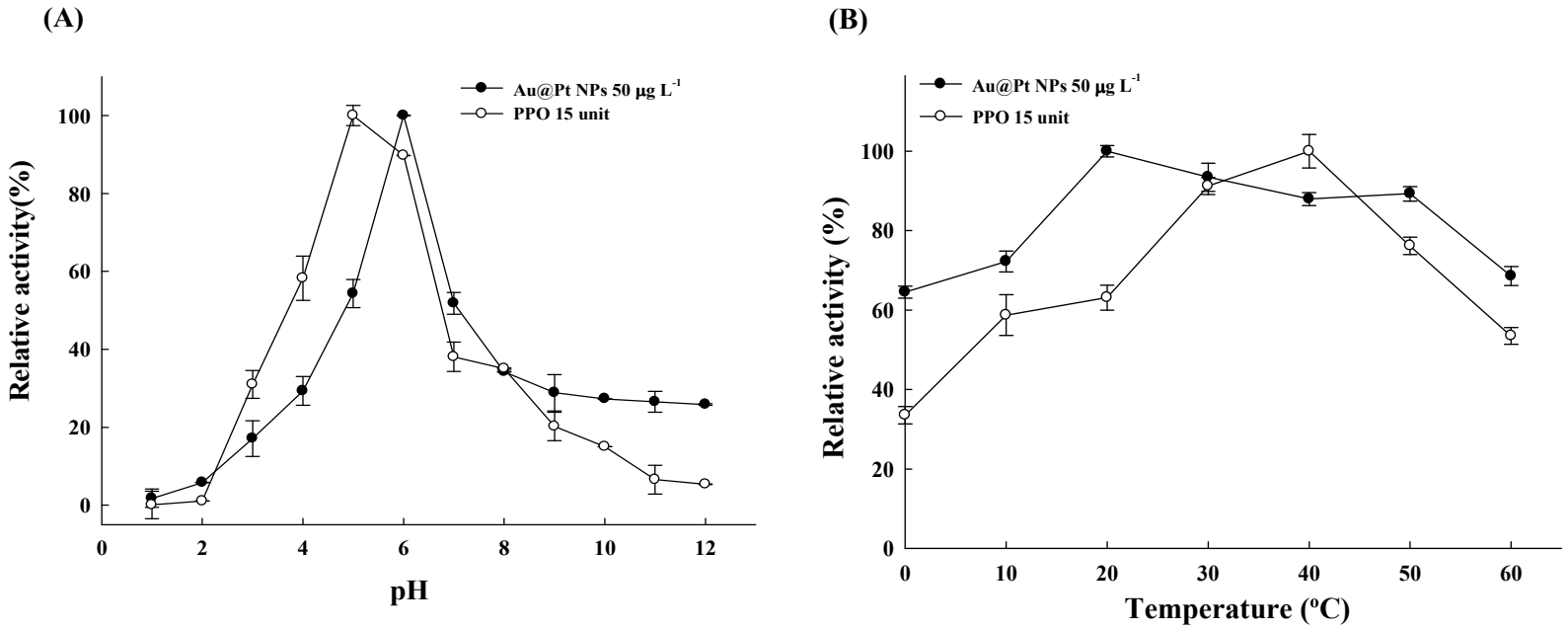

Fig. 5 Polyphenol oxidase (PPO) mimetic activity of Au@Pt nanoparticles (NPs). Effect of pH (A) and temperature (B). The reaction solution included 60 μL of 15 units of PPO or 50 μg L^{-1} of Au@Pt NPs, 180 μL of buffer solution, and 60 μL of 10 mM catechol. Catalytic reactions incubated at different temperatures from 0 to 60 °C were investigated under the optimum pH, respectively. The data are presented as mean ± SD (n = 3).

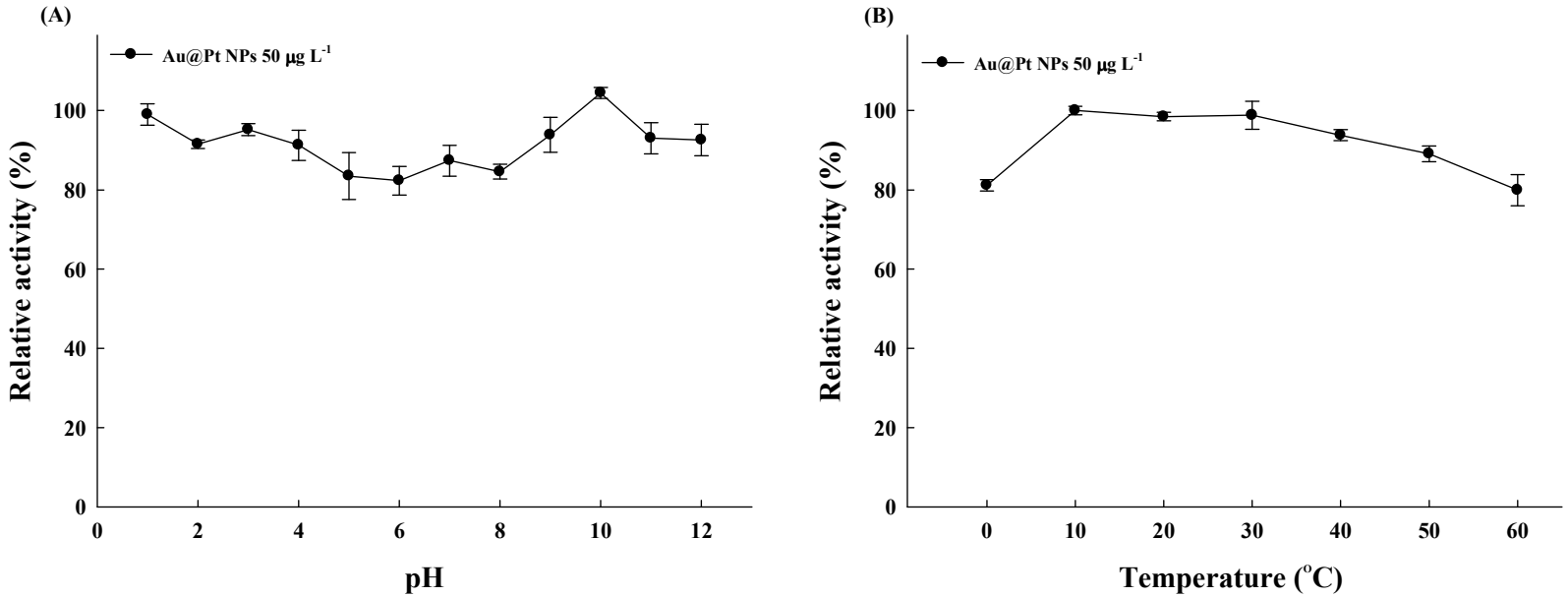

Fig. 6 The stability of Au@Pt nanoparticles (NPs). (A) Au@Pt NPs were incubated at a range of pH values from 1 to 12. (B) Au@Pt NPs were incubated at a range of temperatures between 0 and 60 °C for 2 h, and the polyphenol oxidase activity was measured under standard conditions. The data are presented as mean ± SD (n = 3).

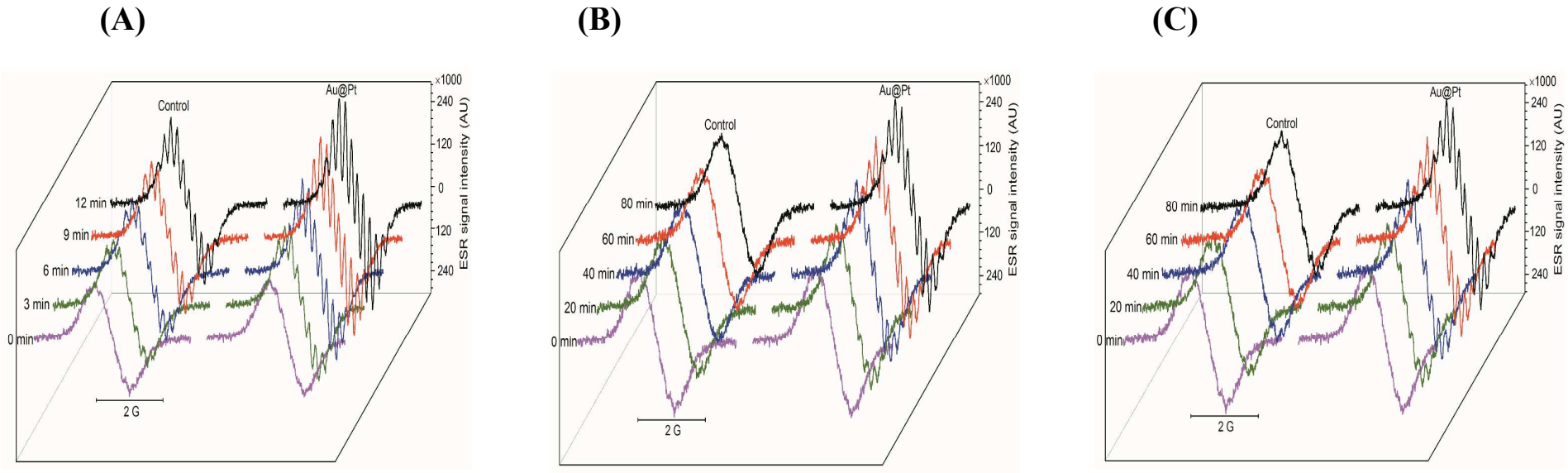

Fig. 7 Evolution of the electron spin resonance (ESR) spectrum of the spin label CTPO during the autoxidation of (A) pyrogallol, (B) L-DOPA, and (C) catechol with or without the presence of Au@Pt. The reaction mixture contained 0.1 mM CTPO and 5 mM pyrogallol, L-DOPA, or catechol in 100 mM PBS (pH 7.4) in the absence or presence of 15 μg L^{-1} Au@Pt.

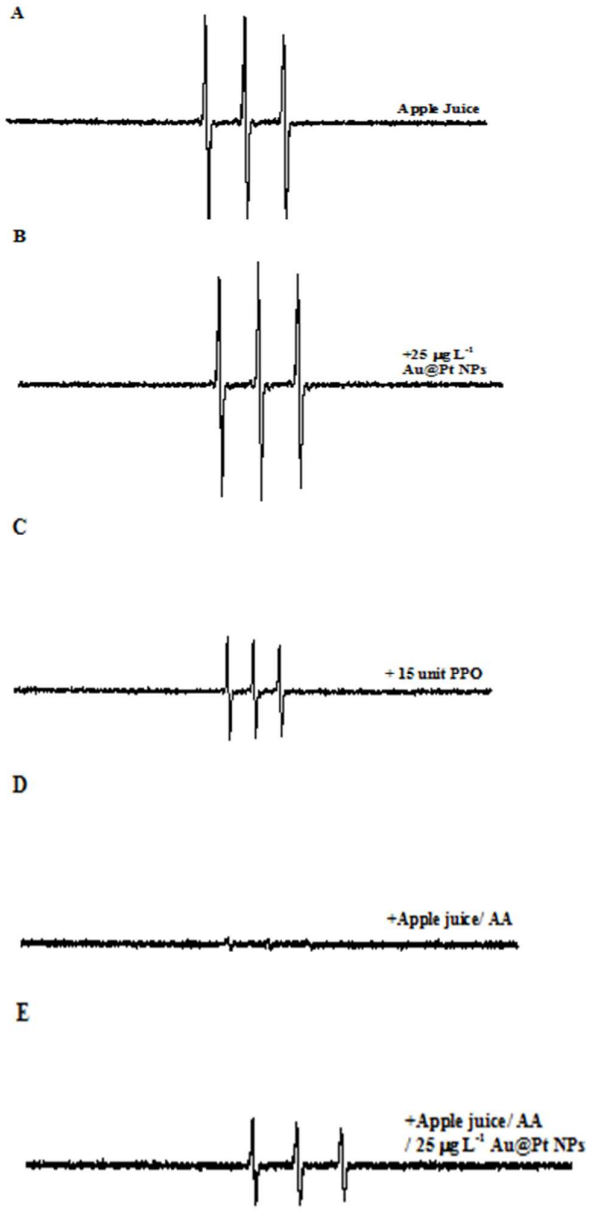

Fig. 8 Evolution of the electron spin resonance (ESR) spectrum of the spin label CTPO during the autoxidation of (A) Apple juice, (B) 25 μg L^{-1} Au@Pt, (C) 15 unit PPO, (D) Apple juice and Ascorbic acid(AA) and (E) Apple juice, AA and 25 μg L^{-1} Au@Pt NPs. The reaction mixture contained 0.1 mM CTPO and 25 μg L^{-1} Au@Pt NPs, 15 units of PPO, or 100 μL apple juice with or without AA (0.1%) and Au@Pt NPs (25 μg L^{-1}) in 100 mM PBS (pH 7.4).

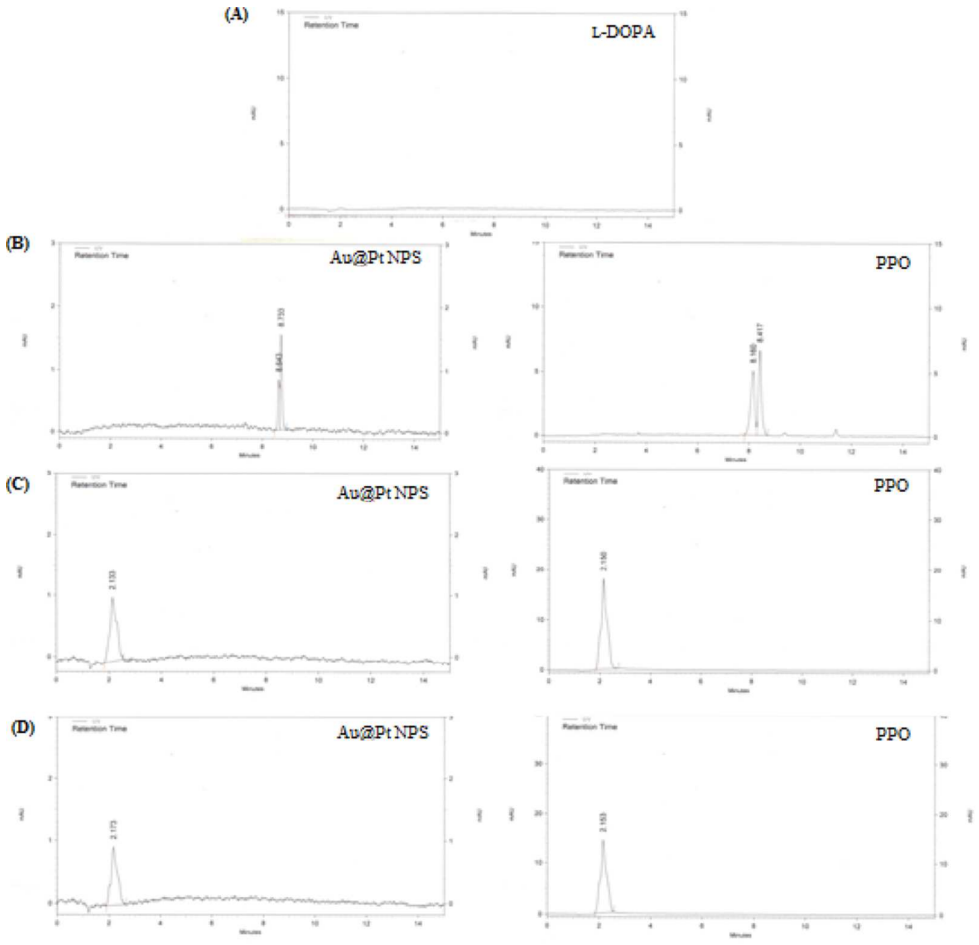

Fig. 9 HPLC chromatograms of (A) L-DOPA and L-DOPA mixed with Au@Pt NPs or PPO with different incubation time for (B) 5 min, (C) 1h, (D) 2 h at 25 °C